NASA Technical Memorandum 102458

On Protection of Freedom's Solar Dynamic Radiator from the Orbital Debris Environment Part 1: Preliminary Analyses and Testing

Jennifer L. Rhatigan
Lewis Research Center
Cleveland, Ohio

Eric L. Christiansen
Lyndon B. Johnson Space Center
Houston, Texas

and

Michael L. Fleming
LTV Missiles and Electronics
Dallas, Texas

Prepared for the
International Solar Energy Conference
sponsored by the American Society of Mechanical Engineers
Miami, Florida, April 1–4, 1990

ON PROTECTION OF FREEDOM'S SOLAR DYNAMIC RADIATOR FROM THE ORBITAL DEBRIS ENVIRONMENT

PART 1: PRELIMINARY ANALYSES AND TESTING

Jennifer L. Rhatigan
National Aeronautics and Space Administration
Lewis Research Center
Cleveland, Ohio

Eric L. Christiansen
National Aeronautics and Space Administration
Lyndon B. Johnson Space Center
Houston, TX

Michael L. Fleming
LTV Missiles and Electronics
Dallas, TX

ABSTRACT

A great deal of experimentation and analysis has been performed to quantify penetration thresholds of components which will experience orbital debris impacts. Penetration had been found to depend upon mission specific parameters such as orbital altitude, inclination, and orientation of the component; and upon component specific parameters such as material, density and the geometry particular to its shielding. Experimental results are highly dependent upon shield configuration and cannot be extrapolated with confidence to alternate shield configurations. Also, current experimental capabilities are limited to velocities which only approach the lower limit of predicted orbital debris velocities. Therefore, prediction of the penetrating particle size for a particular component having a complex geometry remains highly uncertain.

This paper describes the approach developed to assess on-orbit survivability of the solar dynamic radiator due to micrometeoroid and space debris impacts. Preliminary analyses are presented to quantify the solar dynamic radiator survivability, and include the type of particle and particle population expected to defeat the radiator bumpering (i.e., penetrate a fluid flow tube). Results of preliminary hypervelocity impact testing performed on radiator panel samples (in the 6 to 7 km/sec velocity range) are also presented. Plans for further analyses and testing are discussed. These efforts are expected to lead to a radiator design which will perform to requirements over the expected lifetime.

NOMENCLATURE

A	area exposed to micrometeoroid or debris impact, m^2
d	diameter of spherical projectile, mm
h	spacing between plates (double plate model), mm
K	0.57 for aluminum alloy targets 0.38 for 17-4 PH annealed stainless steel
m	particle mass, g
N	flux of particles in particles/(year m^2)
P	probability of no penetration
T	time of exposure to micrometeoroid or debris impact, years
t	thickness of plate (single plate model), cm
t_1	thickness of first plate (double plate model), mm
t_2	thickness of second plate (double plate model), mm
S	spacing between target plates (double plate model), cm
V	normal impact velocity, km/sec
δ_p	particle density, g/cm^3
δ_t	target density, g/cm^3
δ_y	yield stress of second plate (double plate model), $lb/in.^2$

INTRODUCTION

A program is in progress to better understand the environmental threat due to micrometeoroids and space debris to a particular component in low earth orbit--the solar dynamic power module radiator on Space Station Freedom. The prediction of survivability in low earth orbit from micrometeoroids and space debris impacts is challenging due to uncertainties in (1) the determination of the size, mass and velocity of a particle which will penetrate a particular component, and (2) the prediction of the actual debris environment that the component will encounter in terms of type of particle (size and mass), population of particles in

orbit (currently and over the life of a component), and flux of particles (by altitude, velocity, direction, and size).

The objective of the program described herein is to reduce the first of these uncertainties for the solar dynamic radiator. The second of these uncertainties has received much attention in the design of Freedom and is documented in the literature (12).

This paper describes the approach used to assess survivability of the radiator due to this environmental threat, including preliminary analyses of survivability, results of preliminary penetration threshold testing, and plans for future testing.

BACKGROUND

Solar dynamic (SD) power modules provide for the growth power requirements of Freedom. The solar dynamic radiator (SDR) acts as the thermal sink for the Closed Brayton Cycle for the SD power system. Figures 1 and 2 illustrate the SD radiator components and baseline configuration. The multipanel radiator is automatically deployed using a motorized, scissor-arm and cable mechanism. Heat is rejected by pumping a single-phase heat transfer fluid (n-heptane) through the radiator panels, which are plumbed in parallel by flexible hoses. Each radiator panel is configured with inlet and outlet flow manifolds. Flow tubes are connected to manifolds by perpendicular take-offs and run the length of the panel. The SDR contains a redundant flow path, which is to be used in the event of a failure of the primary flow path. The current design calls for 18 active tubes per panel, alternating with 18 secondary (redundant) tubes. The SD power system and radiator are described in detail in Refs. 1 to 3.

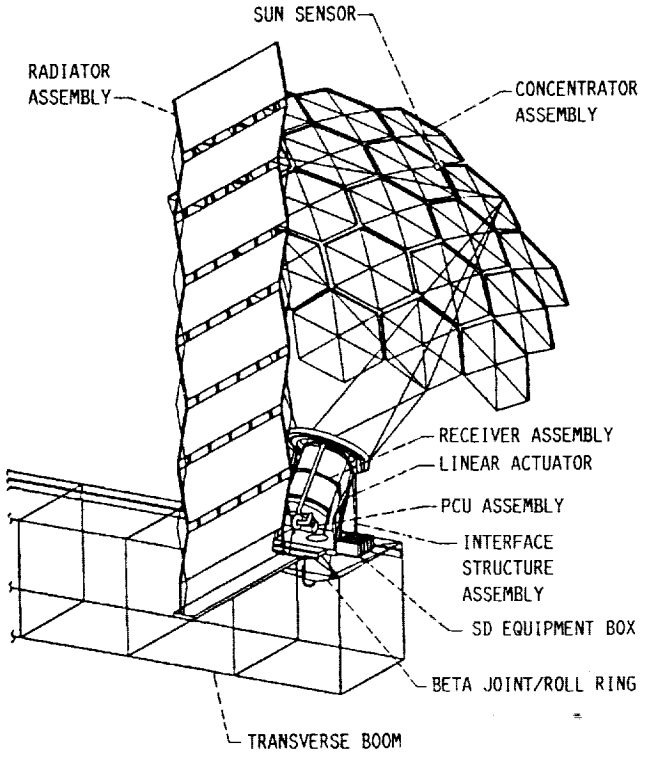

FIGURE 1. - CLOSED BRAYTON CYCLE SOLAR DYNAMIC POWER MODULE.

As can be seen in Fig. 1, the SD radiator is composed of several parts which include the deployment structure, the deployment mechanism, the radiator panels and the plumbing which connects the fluid flow components to the radiator and connects the radiator panels to each other. Impact of a large enough particle could certainly damage the structure and must be considered at some point in the program. However, the current effort has concentrated on the design and analysis for protection of the fluid passages. A puncture of one of the passages in a pumped liquid radiator renders the entire system inoperative (thus

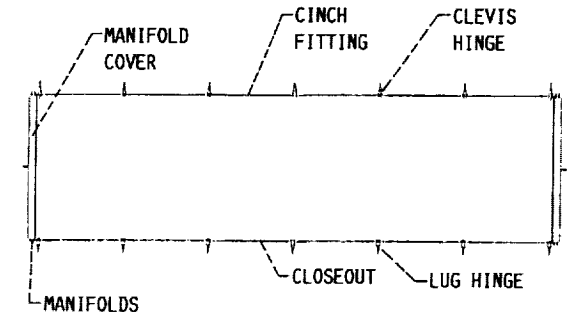

(A) RADIATOR PANEL DESIGN.

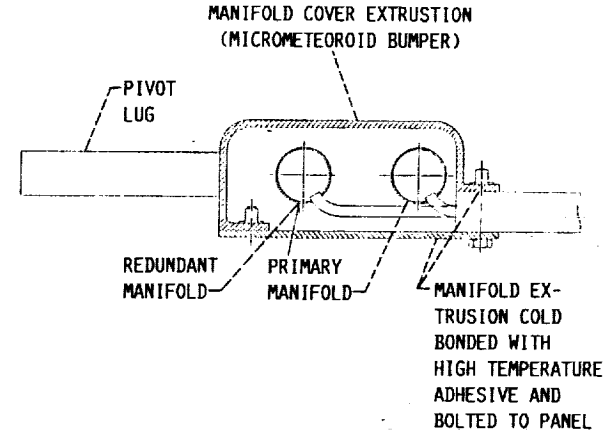

(B) PANEL MANIFOLD DETAILS.

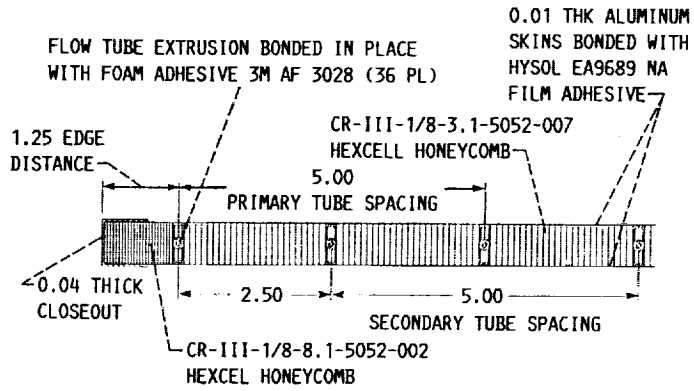

(C) RADIATOR PANEL DETAILS.

FIGURE 2. - DETAILS OF SDR PANEL DESIGNS (ALL DIMENSIONS IN INCHES; 1 INCH = 2.54 CM).

necessitating a redundant system). As a result this aspect of protection is of primary concern.

The heat rejection system requirements call for a 0.95 probability of no loss of heat rejection due to penetration. The SDR is configured with multiple panels in which flow tubes (both primary and secondary) are embedded in a parallel flow path arrangement. Full heat rejection capability (in the secondary fluid loop) is available should the primary fluid loop be penetrated; thus, the probability of no loss of heat rejection due to penetration is reduced to 0.77 for each of the two redundant systems.

PRELIMINARY ANALYSES

The flow tubes are shielded by a bumpered configuration to reduce vulnerability to penetration by micrometeoroids and space debris in the low-earth-orbit environment (Fig. 2). The fluid system also includes panel manifolds (Figs. 1 and 2), flex hoses (Fig. 3), and conventional, 1.0 in. i.d. hard tube plumbing (in the base structure and first elements of the deployment mechanism). Each of these components presents a different target, and thus a different penetration configuration, for impact of a particle. Available analytical techniques from the literature are all based on empirical data from tests of two simple configurations: single sheet impacts and multiple, parallel sheet impacts. The SDR design incorporates shielding geometries which, in some cases, pose complex projectile paths for penetration of a particle into the fluid loop. For instance, projectiles traveling towards a panel flow tube at an angle that is not perpendicular to the plane of the panel can encounter the panel facesheet, honeycomb and some portion of the bumpered extrusion. To justify applications of the available analytical techniques to the more complex penetration geometries is not attempted; however, the equations were used to obtain an initial evaluation for the purpose of establishing the overall SDR vulnerability and to identify areas where design changes were required. In this limited role the analysis was highly effective.

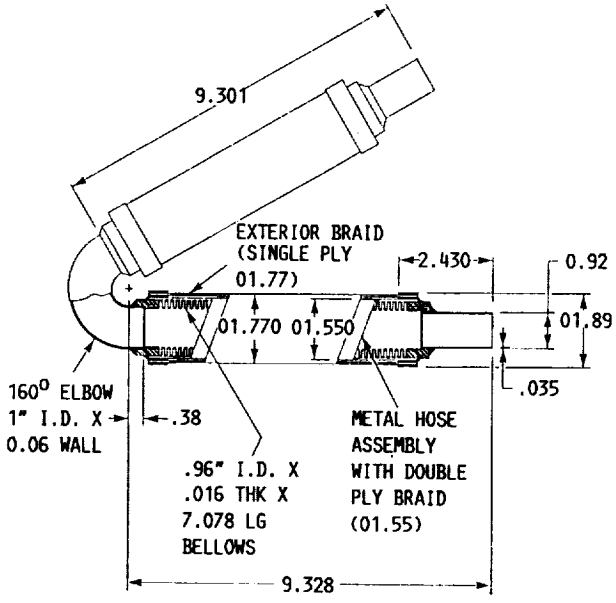

FIGURE 3. - SDR FLEX HOSE DESIGN (ALL DIMENSIONS IN INCHES, 1 INCH = 2.54 CM).

The literature was surveyed and two techniques were selected for use in analysis of the components where the penetration path is composed of more than one surface (parallel sheets). These two techniques were:

$$d = \left[0.00288\ V^{-1}\ t_1^{1.9}\ t_2^{3.6} (\delta_t/\delta_p)^{1.8}\ h^{5}\right]^{(1/10.5)} \quad (1)$$

$$d = 20\ V^{-1}\ t_2 (\pi\ \delta_p/6)^{-1/3}\ (\delta_p/\delta_t)^{-1/6}\ (S\ \delta_y/50\ 000)^{1/2} \quad (2)$$

where 50 000 is yield stress of the 2024-T3 aluminum target. Equation (1) is a modification of the equation developed in Ref. 4 and Eq. (2) a modification of the equation developed in Ref. 5. The equations were modified to include a ratio of particle to target density for materials other than those tested. Equation (2) was modified to include the handbook value for the yield stress of 2024-T3 aluminum. Equation (2) consistently predicts smaller diameter particles for penetration. Both equations are empirically derived, so differences in predictions are thought to be due to differences in the experiments.

For components where a single sheet is penetrated, the equation given below was employed (5):

$$t = K\ m^{0.352}\ v^{0.875} \quad (3)$$

Once the diameter or mass of the particle which would just penetrate the single sheet component is calculated, the frequency of impact of these size particles (or larger particles) was taken from JSC 20 000 for debris and NASA SP 8013 for micrometeoroid. It should be noted that penetration of any portion of the primary flow loop would cause a fluid leak in that loop and necessitate use of the redundant (secondary) flow loop; thus, penetration of the flow loop is the design criteria of interest. The probability of no penetration is calculated from:

$$P = e^{-NAT} \quad (4)$$

Analysis of the initial SDR configuration resulted in probability of less than 1 percent survival. Analysis of the components individually indicated the unprotected hard lines and flex hoses were the cause of the low survival rate. The design was modified to add bumper protection of the hard tube and an additional layer of braided aluminum on the flex hoses. This dramatically increased the overall survival rate to greater than the 0.95 requirement at a cost of a slight mass increase. While the confidence in application of the analytical techniques to the complex configurations of the SDR components was not sufficient to recommend their use for design verification, they did serve to identify the areas of the design which required modification.

PRELIMINARY TESTING

The unique geometry of the SDR flow tubes necessitated a preliminary set of hypervelocity impact tests to assess the applicability of empirical data for simpler geometries. The NASA Johnson Space Center (JSC) Hypervelocity Impact Research Laboratory (HIRL) was selected for this initial phase of solar dynamic radiator system tests.

Test Facility

The JSC HIRL contains three two-stage, light-gas launchers. A single gun was used in this study which has a 4.3 mm launch tube bore and is capable of launching 3.2 mm diameter aluminum spheres and 73 mg nylon slugs at over 7 km/sec. Additional details of the capabilities of the HIRL launchers are described in other reports (7-9).

The hypervelocity impact tests were supported by a Cordin Model 330 IR high-speed framing camera. It operates at 1 M frames/sec with a 5 ns exposure time (10). The camera provides data on projectile velocity and integrity, and ejected particle pattern and velocity. It also serves as an important diagnostic tool to confirm that a shot is clean; that just the projectile and no secondary particles (such as fragments of sabot, shear plate, or other gun debris) hit the target, or to provide clues to the problem if the shot is not clean.

Test Procedure

Twelve hypervelocity impact tests were conducted on target specimens representative of the solar dynamic radiator panels (Fig. 2). Each test specimen was approximately 5.1 cm wide by 6.0 cm long by 1.8 cm thick and was bisected by a single bumpered flow tube. Test conditions are given in Table I. The objective for these preliminary tests was to assess the response of the radiator panels to hypervelocity impact as a function of projectile diameter and impact angle. In particular, it was hoped the tests would help determine the "ballistic limit" of the flow tubes within the panels; that is, the particle size that just causes failure (penetration) of the flow tubes.

Because orbital debris is expected to have the density of aluminum in the particle size range tested (11,12), aluminum projectiles were used in the impact tests. Aluminum (A12017) spheres with diameters of 1.0 mm, 1.25 mm, and 1.6 mm were launched at impact angles normal (0°) and at 45° to the panel surface. In all but one of the 45° angle impact tests, the projectile flight direction was directed perpendicular to the panel flow tube's longitudinal axis. One 45° angle shot was directed parallel to the flow tube longitudinal axis. These angles were selected to provide data for normal and oblique impacts, and are not necessarily critical angles.

The tests were conducted in a narrow range of impact velocities (6 to 7 km/sec). These velocities only approach the lower limit of the velocities expected on orbit, but are currently the highest velocities available experimentally in the particle range of interest. Some method is needed to scale the experimental results to velocities experienced on-orbit. Average impact velocities for orbital debris and meteoroids are 10 and 20 km/sec, respectively (11-13). For simplified hazard assessments using the preliminary laboratory test results, scaling to higher impact velocities expected on-orbit can be accomplished by empirical penetration equations for single and dual-sheet aluminum structures published in the literature (14,15). These empirical models have limited applicability to this particular case since the geometry of the radiator panels is more complicated than the bases of the empirical models (given the internal honeycomb and nonparallel aluminum plates contained within the radiator panel elements). Therefore, later phases of the radiator system testing could involve tests at several impact velocities.

TABLE I. - HYPERVELOCITY IMPACT TEST DATA FOR SOLAR DYNAMIC RADIATOR PANELS

Projectile parameters[a]							Target damage		
HIRL shot number	Material	Diameter, mm	Velocity, km/s	Impact angle, degree	Direction relative to flow axis	Mass, mg	Miss distance aim line to middle flow tube, mm	Bumper interior damage comments	Flow tube damage comments
A873	A12017-T4	1.0	6.9	45	Normal	1.46	13.1	----------	-------
A875	↓	↓	7.0	0	--------	↓	7.0	----------	-------
A876	↓	↓	6.73	45	Normal	↓	3.2	Slight dimple	-------
A877	↓	↓	6.85	0	--------	↓	2.4	Spall bubble	-------
A880	↓	↓	6.8	45	Normal	↓	8.5	----------	-------
A882	↓	↓	5.9	↓	↓	↓	0.5	----------	-------
A883	↓	↓	6.90	↓	↓	↓	(n/a)	----------	-------
A884	↓	↓	7.04	↓	↓	↓	3.5	Slight dimple	-------
A885	↓	↓	6.7	↓	Parallel	↓	5.2	----------	-------
A891	A12017-T6	1.59	6.94	↓	Normal	5.86	2.4	Perforated	Pinched
A892	A12017-T6	1.59	6.67	0	--------	5.86	1.2	Perforated	Pinched
A897	A12017-T4	1.25	6.77	45	Normal	2.86	9.2	----------	-------

[a]All spherical projectiles with density 2.796 g/cc.

TEST RESULTS

Figure 4 shows the results of a 1.0 mm aluminum sphere impacting at a normal angle (0°) at 6.85 km/sec. Although the projectile missed striking the flow tube directly, it left a "spall bubble" on the inside of the flow tube bumpering (the flow tube was unaffected).

Each shot was aimed at the center of the flow tube, although some "miss distance" occurred for each shot due to experimental limitations (e.g., Fig. 4 shows the projectile hole to one side of the flow tube axis). The miss distance shown in Table I is the minimum distance from the projectile flight path to the middle of the flow tube. Since the nominal o.d. of the flow tube is 3.4 mm (0.134 in.), miss distances greater than 1.7 mm do not intersect the flow tube. Only two shots (A882 and A892) had original trajectories that would have impacted the flow tube.

Figure 5 shows the results of a 1.6 mm aluminum sphere impact at a normal (0°) impact angle. This impact was nearly centered over the flow tube (1.2 mm miss distance on a 1.7 mm radius flow tube). The projectile broke up when it impacted the top of the flow tube bumper, and the expanding debris cloud from the initial impact penetrated one side and deformed the other side of the flow tube bumper. Although the impact left a hole in the side of the bumper and partially pinched-off the flow tube (restricting flow), it did not penetrate into the flow tube itself. However,

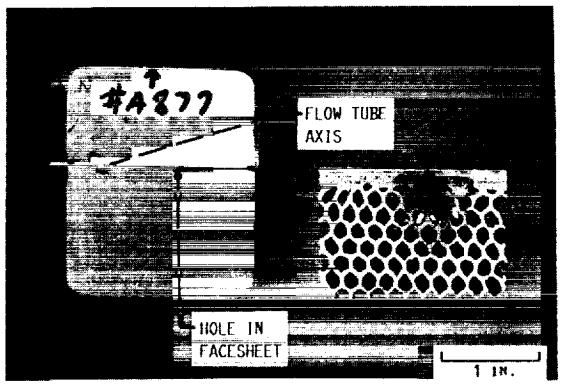

(A) FACESHEET AND HONEYCOMB.

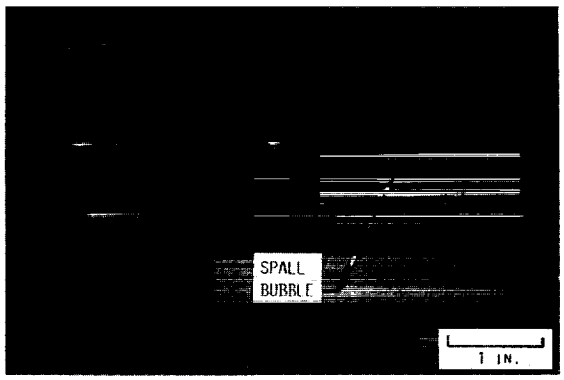

(B) FLOW-TUBE CROSS SECTION.

FIGURE 4. - PHOTOGRAPHIC DOCUMENTATION OF JSC HIRL SHOT A877 (1.0 MM AL 2017-T4 PROJECTILE, 6.85 KM/SEC, NORMAL IMPACT ANGLE).

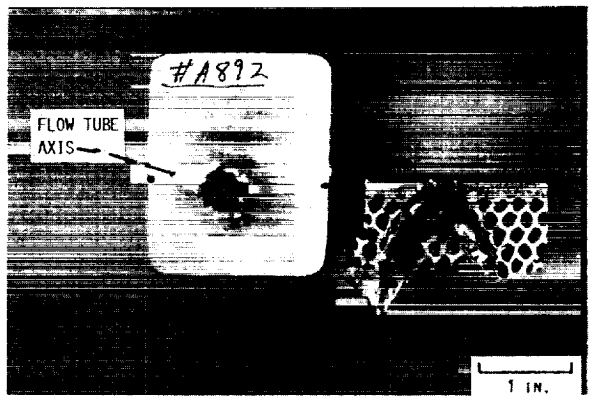

(A) FACESHEET AND HONEYCOMB.

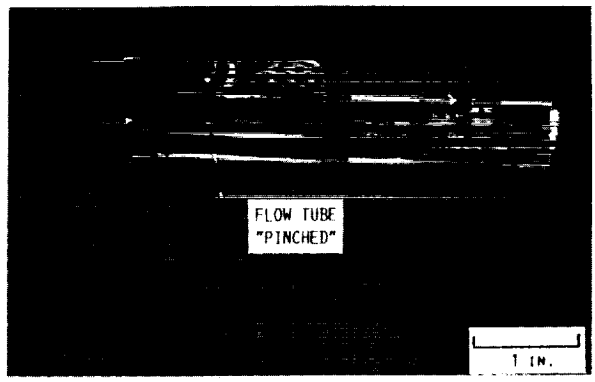

(B) FLOW-TUBE CROSS-SECTION.

FIGURE 5. - PHOTOGRAPHIC DOCUMENTATION OF JSC HIRL A892 (1.59 MM AL 2017-T6 PROJECTILE, 6.67 KM/SEC, NORMAL IMPACT ANGLE).

as shown in Fig. 6, a very large hole was opened into the flow tube bumper wall for the same size projectile (1.6 mm) at a 45° impact, which if better centered on the flow tube (miss distance was 2.4 mm), would most likely have penetrated into the flow tube as well.

With these experimental results, a preliminary hazard assessment can be performed for the radiator panel flow tubes. The critical particle size causing failure of the second sheet (d) is inversely proportional to both projectile velocity and the square root of particle density by the Cour-Palais penetration function for a dual-wall aluminum structure (15), i.e.:

$$d \propto V^{-1} \delta_p^{-0.5} \qquad (5)$$

Given that a 1.59 mm aluminum particle at 6.9 km/sec will penetrate a flow tube, it was calculated that a 1.09 mm debris particle (with average velocity of 10 km/sec, density of 2.8 g/cc) and a 1.30 mm meteoroid particle (average velocity of 20 km/sec, density of 0.5 g/cc) will also cause failure. (It should be noted that the calculation was based on the results of a single data point. Future testing will examine the penetration limit in more detail.)

There are two independent flow loops for the solar dynamic radiator system. Each of eight radiator panels in the solar dynamic system is 8.05 m long and contains 18 lengths of primary flow tubes (3.4 mm o.d.) in each cooling loop for a total area of both primary and secondary loops of 24.78 m^2. A preliminary estimate of the number of impacts from orbital debris and meteoroids on the radiator panel tubes that are large enough to cause failure over a 10 year period is given in Table II. These numbers were calculated using the currently baselined space station orbital debris (11) and meteoroid (13) environments. Table II shows that the probability of no-failure of either of the two loops from orbital debris and meteoroids is 0.67 over 10 years (i.e., there is one chance in three that one of the two loops will fail in 10 years). This was calculated from the individual probability of no-failure of the primary and secondary loops which are both 0.816 over 10 years (i.e., $0.816^2 = 0.67$). The chance that both primary and secondary loops will not fail from meteoroids and debris over 10 years is 0.966.

Figure 7 illustrates the high-speed camera film from HIRL shot A891 (oblique 45° impact of a 1.59 mm aluminum sphere at 6.94 km/sec). A large trash particle visible in the high-speed film following the projectile in shot A891 did not result in much target damage as indicated in Fig. 6 (it barely penetrated the face sheet). The high-speed camera film from shot A877 (normal impact of a 1.0 mm aluminum sphere at 6.85 km/sec) is given in Fig. 8. This was a clean

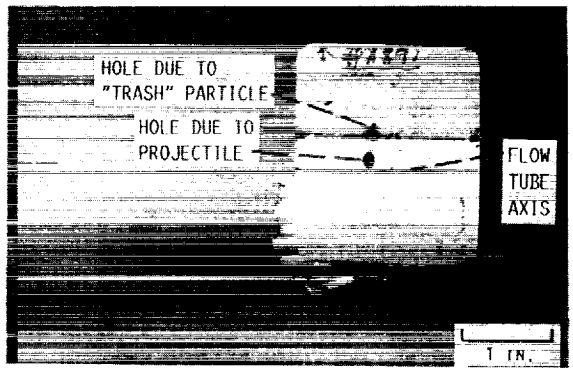

(A) FRONT OF PANEL FACESHEET.

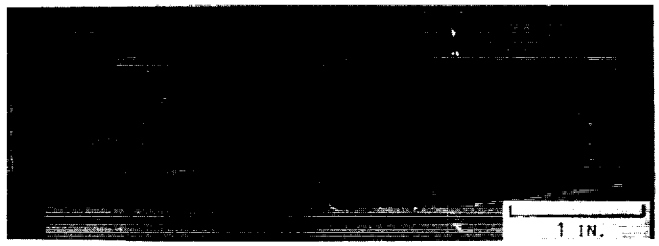

(B) FLOW-TUBE CROSS-SECTION.

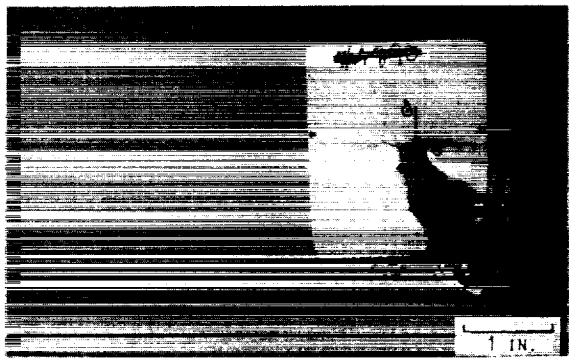

(C) BACK OF PANEL FACESHEET.

FIGURE 6. - PHOTOGRAPHIC DOCUMENTATION OF JSC HIRL SHOT A891. (1.59 MM AL 2017-T6 PROJECTILE, 6.94 KM/SEC, 45° IMPACT ANGLE).

TABLE II. - METEOROID/DEBRIS IMPACTS ON SOLAR DYNAMIC RADIATOR PANEL TUBES[a]

[Surface area: 12.39 m^2 per loop (24.78 m^2 for both loops); life: 10 years; Altitude: 500 km; critical meteoroid particle size: 0.130 cm; critical debris particle size: 0.109 cm.]

Radiator case	Surface area, m^2	Critical particle flux, impacts/m^2-year		Number of critical impacts over life			Probability of no-failure
		Meteoroid	Debris	Meteoroid	Debris	Combined	
Single loop	12.39	7.27E-4	9.14E-4	0.09	0.113	0.203	0.816
Either loop (without redundancy)	24.78	↓	↓	.18	.227	.407	.666
Both loops (with redundancy)	24.78	↓	↓	----	-----	.034	.966

[a]Based on current debris model in Ref. 11 and meteoroid model in Ref. 13.

FIGURE 7. - HIGH-SPEED CAMERA FILM OF JSC HIRL SHOT A891 (1.59 MM AL 2017-T6 SPHERE, 6.94 KM/SEC, 45^{0} IMPACT ANGLE). (1 MICRO-SECOND BETWEEN FRAMES).

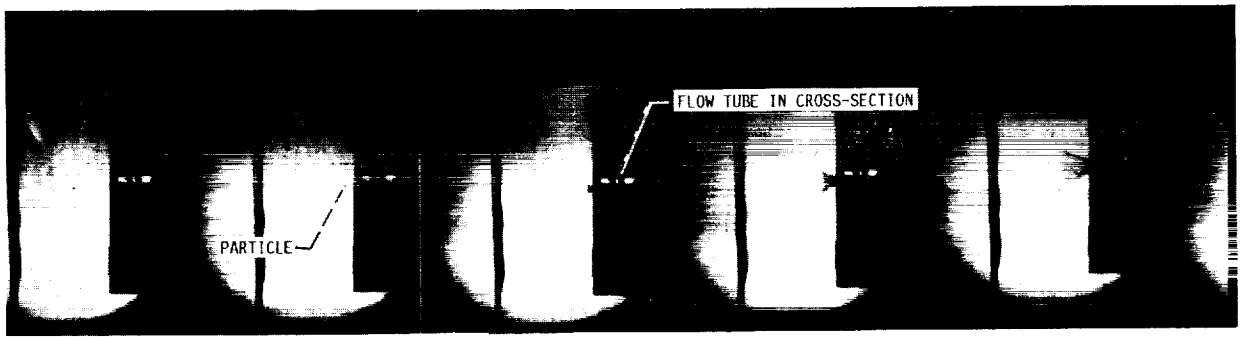

FIGURE 8. - HIGH-SPEED CAMERA FILM OF JSC HIRL SHOT A877 (1.0 MM AL 2017-T4 SPHERE, 6.85 KM/SEC, NORMAL 0^{0} IMPACT). (1 MICRO-SECOND BETWEEN FRAMES).

shot as shown in the film and by the target record (Fig. 4).

Two additional (and unexpected) observations were made during post-test analyses. Firstly, the aluminum honeycomb appears to provide indirect protection for the flow tube. In a number of test cases, the honeycomb channelled the particle through the panel. This would tend to reduce the number of oblique impacts that would reach the flow tube after passing through the honeycomb. Secondly, the foam adhesive which binds the honeycomb to the flow tube extrusion also had a similar beneficial effect in providing additional protection from oblique impacts.

FUTURE TESTING AND ANALYSES

As previously discussed, the equations for penetration analysis were based on results from tests of simple configurations and may not be applicable to more complex geometries such as those of the panel flow tubes and flex hose. As a result, hypervelocity impact testing of these two components are planned at the JSC HIRL facility to determine the size of particle which can be expected to not produce penetration in low earth orbit and thereby the probability of survival.

The preliminary set of tests (described herein) on the panel flow tubes indicated the flow tube is extremely difficult to hit due to the small target size (i.e., 3.4 mm o.d.). As a result, samples were designed which would increase target size but maintain a realistic penetration path. The samples designed for these tests are shown in Fig. 9. Sample A provides a large target for impacts of the flow passage from the side, in order to test the bumper wall effectiveness. Two wall thicknesses will be tested on this sample design. Sample B is designed to increase the target area for impacts directly above the flow passage (and normal to the facesheet) since this was the most difficult angle in preliminary testing. Sample C is a segment of the actual panel design. The test plan is to conduct most of the testing on the easier to hit samples A and B and then to utilize those results to define final penetration limit tests against the actual panel design.

These results can be analyzed to determine the panel flow passage vulnerability through adjustments for particle density and velocity to account for the differences in test conditions and the low-earth-orbit micrometeoroid and debris environment. Testing will be conducted at several approach angles since the penetration path differs for different angles. Testing also will be performed using projectiles with a density nearer to typical micrometeoroid density (0.5 gm/cc) as well as with aluminum projectiles.

These tests are planned for the early 1990 time period. Similar testing of the braided portion of the flex hose are planned for the 1992 time period. The results of these tests will be used in a more rigorous calculation of system reliability. Based on the results of these tests and analyses the design will be modified as required to meet the overall protection requirements.

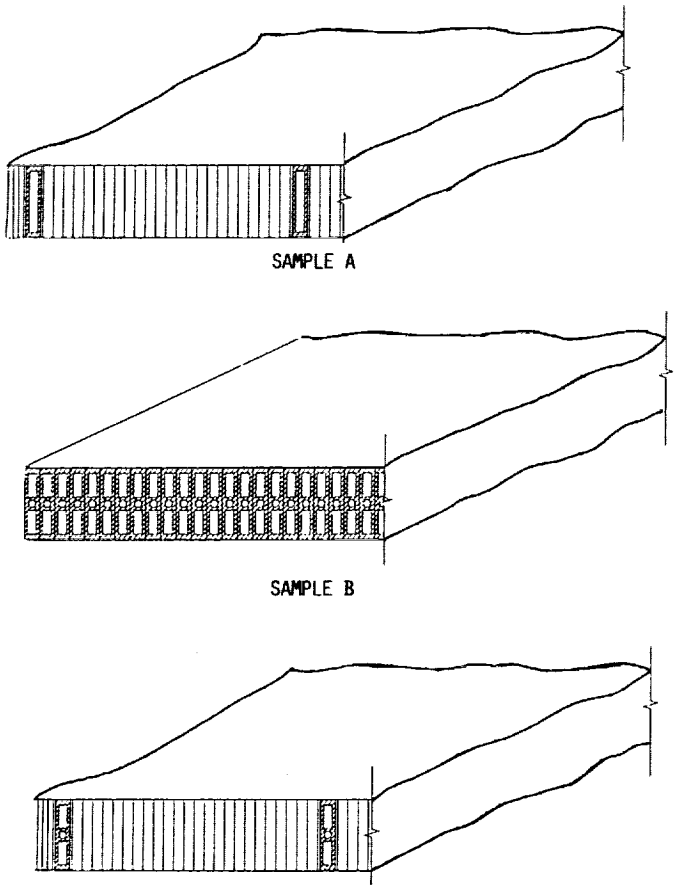

FIGURE 9. - DESIGN OF HYPERVELOCITY TEST SAMPLES TO MAXIMIZE USEFUL TEST RESULTS.

SUMMARY AND CONCLUSIONS

1. A series of 12 hypervelocity impact tests have been performed on representative solar dynamic radiator panel elements. The tests were performed with aluminum spheres having diameters of 1.0 to 1.6 mm, velocities of 6 to 7 km/sec, and impact angles up to 45°. The tests showed that the radiator panel tubes would be penetrated by 1.6 mm diameter particles impacting at laboratory velocities (~7 km/sec).

2. Using current Space Station environment models (11-13), the panel tubes in the baseline solar dynamic radiator system have a 0.966 reliability (with redundancy) from failure by meteoroid and debris impacts over 10 years. However, if the radiator system is replaced after a single loop failure, the calculated radiator probability of no-replacement due to impact failure drops to 0.67 over 10 years.

3. The radiator system is made up of more than just the panel tubes. The reliability of the radiator panel interconnect lines and other subsystems exposed to the meteoroid/debris environment will be determined by hypervelocity impact testing and/or analysis, and the results included in an assessment of the overall radiator system reliability.

4. It should be noted that an updated orbital debris environment has been developed from the latest ground-based measurements and returned spacecraft materials (12). This updated environment is much more severe than the current debris environment (11). These conclusions should be updated when the new debris environment (12) is baselined for Freedom's use.

5. The design of the SD heat rejection system will be modified as necessary to meet the overall protection requirements.

ACKNOWLEDGMENTS

The progress towards understanding the SD radiator survivability in the orbital debris environment is a result of effort on the part of many people. The authors would like to express appreciation to Kerry McLallin of NASA Lewis Research Center, Rick Howerton and Cheng Lu of Rocketdyne, and Jeanne Crews and Burt Cour-Palais of NASA Johnson Space Center for their contributions to this work.

REFERENCES

1. Secunde, R., Labus, T.L., and Lovely, R.G., 1989, "Solar Dynamic Power Module Design," Proceedings of the 24th International Energy Conversion Engineering Conference, Vol. 1, IEEE, Piscataway, NJ, pp. 299-307.
2. McLallin, K.L., et al., 1988, "The Solar Dynamic Radiator With a Historical Perspective," Proceedings of the 23rd International Energy Conversion Engineering Conference, Vol. 3, ASME, pp. 335-340.
3. Fleming, M.L. and Hoehn, F., 1987, "Radiator Selection for Space Station Solar Dynamic Power Systems," Proceedings of the 22nd International Energy Conversion Engineering Conference, Vol. 1, AIAA, pp. 208-213.
4. Nysmith, C.R., 1969, "An Experimental Impact Investigation of Aluminum Double-Sheet Structures," AIAA Paper 69-375.
5. Cour-Palais, B.G., 1979, "Space Vehicle Meteoroid Shielding Design," Comet Halley Micrometeoroid Hazard Workshop, ESA-SP-153, N. Longdon, ed., European Space Agency, Paris, France, pp. 85-92.
6. Frost, V.C., et. al., 1970, "Meteoroid Damage Assessment--Space Vehicle Design Criteria," NASA SP-8042.
7. Christiansen, E.L., 1988, "Investigation of Hypervelocity Impact Damage to Space Station Truss Tubes," Eagle Engineering Report No. 88-176, Houston, TX.
8. Christiansen, E.L., 1987, "Evaluation of Space Station Meteoroid/Debris Shielding Materials," Eagle Engineering Report No. 87-163, Houston, TX.
9. Yew, C.H., Wang, C.Y., and Crews, J.L., 1987, "A Phenomenological Study of the Effect of Hypervelocity Impacts on Graphite-Epoxy Plates," Space Station Freedom Office, NASA Johnson Space Center.
10. Parker, V.C. and Crews, J.L., 1988, "Hypervelocity Impact Studies Using a Rotating Mirror Framing Laser Shadowgraph Camera," High Speed Photography, Videography, and Photonics V, H.C. Johnson, ed., SPIE, Bellingham, WA, pp. 88-95.
11. Kessler, D.J., 1984, "Orbital Debris Environment for Space Station," JSC-20001, NASA Johnson Space Center.
12. Kessler, D.J., Reynolds, R.C., and Anz-Meador, P.D., 1989, "Orbital Debris Environment for Spacecraft Designed to Operate in Low Earth Orbit," NASA TM-100471.
13. 1987, "Space Station Program Natural Environment Definition for Design," NASA Space Station Program Office, JSC-30425.
14. Cour-Palais, B.G., 1987, "Hypervelocity Impact in Metals, Glass and Composites," International Journal of Impact Engineering, Vol. 5, pp. 221-237.
15. Cour-Palais, B.G., 1969, "Meteoroid Protection by Multiwall Structures," AIAA Paper 69-372.

NASA
National Aeronautics and Space Administration

Report Documentation Page

1. Report No.	2. Government Accession No.	3. Recipient's Catalog No.
NASA TM-102458		

4. Title and Subtitle

On Protection of Freedom's Solar Dynamic Radiator from the Orbital Debris Environment
Part 1: Preliminary Analyses and Testing

5. Report Date

6. Performing Organization Code

7. Author(s)

Jennifer L. Rhatigan, Eric L. Christiansen, and Michael L. Fleming

8. Performing Organization Report No.

E-5245

10. Work Unit No.

474-10-52

9. Performing Organization Name and Address

National Aeronautics and Space Administration
Lewis Research Center
Cleveland, Ohio 44135-3191

11. Contract or Grant No.

13. Type of Report and Period Covered

Technical Memorandum

12. Sponsoring Agency Name and Address

National Aeronautics and Space Administration
Washington, D.C. 20546-0001

14. Sponsoring Agency Code

15. Supplementary Notes

Prepared for the International Solar Energy Conference sponsored by the American Society of Mechanical Engineers, Miami, Florida, April 1-4, 1990. Jennifer L. Rhatigan, NASA Lewis Research Center; Eric L. Christiansen, NASA Lyndon B. Johnson Space Center, Houston, Texas; Michael L. Fleming, LTV Missiles and Electronics, Dallas, Texas.

16. Abstract

A great deal of experimentation and analysis has been performed to quantify penetration thresholds of components which will experience orbital debris impacts. Penetration had been found to depend upon mission specific parameters such as orbital altitude, inclination, and orientation of the component; and upon component specific parameters such as material, density and the geometry particular to its shielding. Experimental results are highly dependent upon shield configuration and cannot be extrapolated with confidence to alternate shield configurations. Also, current experimental capabilities are limited to velocities which only approach the lower limit of predicted orbital debris velocities. Therefore, prediction of the penetrating particle size for a particular component having a complex geometry remains highly uncertain. This paper describes the approach developed to assess on-orbit survivability of the solar dynamic radiator due to micrometeoroid and space debris impacts. Preliminary analyses are presented to quantify the solar dynamic radiator survivability, and include the type of particle and particle population expected to defeat the radiator bumpering (i.e., penetrate a fluid flow tube). Results of preliminary hypervelocity impact testing performed on radiator panel samples (in the 6 to 7 km/sec velocity range) are also presented. Plans for further analyses and testing are discussed. These efforts are expected to lead to a radiator design which will perform to requirements over the expected lifetime.

17. Key Words (Suggested by Author(s))	18. Distribution Statement
Space radiator; Hypervelocity impact; Survivability; Solar dynamic power; Space debris; Micrometeroids; Space environment	Unclassified – Unlimited Subject Category 20

19. Security Classif. (of this report)	20. Security Classif. (of this page)	21. No. of pages	22. Price*
Unclassified	Unclassified	10	A02

NASA FORM 1626 OCT 86

*For sale by the National Technical Information Service, Springfield, Virginia 22161